Kitaev-Heisenberg models for iridates on the triangular, hyperkagome, kagome, fcc, and pyrochlore lattices

Itamar Kimchi[1] and Ashvin Vishwanath[1,2]
[1]*Department of Physics, University of California, Berkeley, California 94720, USA*
[2]*Materials Science Division, Lawrence Berkeley National Laboratories, Berkeley, California 94720, USA*
(Received 5 June 2013; revised manuscript received 17 December 2013; published 15 January 2014)

The Kitaev-Heisenberg (KH) model has been proposed to capture magnetic interactions in iridate Mott insulators on the honeycomb lattice. We show that analogous interactions arise in many other geometries built from edge-sharing IrO_6 octahedra, including the pyrochlore and hyperkagome lattices relevant to Ir_2O_4 and $Na_4Ir_3O_8$, respectively. The Kitaev spin liquid exact solution does not generalize to these lattices. However, a different, exactly soluble point of the honeycomb lattice KH model, obtained by a four-sublattice transformation to a ferromagnet, generalizes to all of these lattices and even to certain additional further neighbor Heisenberg couplings. A Klein four-group $\cong\mathbb{Z}_2\times\mathbb{Z}_2$ structure is associated with this mapping (hence *Klein duality*). A finite lattice admits the duality if a simple geometrical condition is met. This duality predicts fluctuation-free ordered states on these different 2D and 3D lattices, which are analogues of the honeycomb lattice KH *stripy* order. This result is used in conjunction with a semiclassical Luttinger-Tisza approximation to obtain phase diagrams for KH models on the different lattices. We also discuss a Majorana fermion based mean-field theory at the Kitaev point, which is exact on the honeycomb lattice, for the KH models on the different lattices. We attribute the rich behavior of these models to the interplay of geometric frustration and frustration induced by spin-orbit coupling.

DOI: 10.1103/PhysRevB.89.014414 PACS number(s): 75.10.Jm

I. INTRODUCTION

Long viewed as a perturbative correction, relativistic spin-orbit coupling has in recent years been increasingly asserting its role within condensed matter physics. It took center stage with topological insulators, time-reversal invariant states of electrons with no strong interactions that use spin-orbit coupling to generate nontrivial topology in the band structure [1–3]. Electron correlations may amplify [4,5] the effects of spin-orbit coupling (SOC), enriching the taxonomy of possible phases. Thus Mott insulating states of heavy magnetic ions could realize novel Hamiltonians, which may be hitherto unexplored or not thought to describe real materials.

One such $S=1/2$ Hamiltonian has been proposed by Jackelli and Khaliullin [6,7] to occur in the honeycomb iridates Na_2IrO_3 and Li_2IrO_3. It includes the Kitaev exchange, a nearest-neighbor Ising coupling of spin component $\gamma\in\{x,y,z\}$ set by the spatial orientation of the bond [8,9]. The pure Kitaev honeycomb Hamiltonian is exactly solvable with a quantum spin liquid (QSL) ground state of a gapless Majorana coupled to $\mathbb{Z}_2$ fluxes [9]. The proposed magnetic model for these iridates includes the Kitaev as well as SU(2) symmetric Heisenberg coupling, yielding the Kitaev-Heisenberg $S=1/2$ Hamiltonian [7]. It may be written as

$$H_{\mathrm{KH}}=\sum_{\langle ij\rangle}\eta\left[(1-|\alpha|)\vec{S}_i\cdot\vec{S}_j-2\alpha S_i^{\gamma_{ij}}S_j^{\gamma_{ij}}\right] \qquad (1)$$

with $\eta=\pm1$ and $-1\leqslant\alpha\leqslant1$. Here, η sets the sign of Heisenberg exchange, and negative α gives the same sign for both exchanges. Pairs of endpoints of the two α segments for $\eta=+1,-1$ are identified as a single point by the product $\eta\alpha=+1$ (FM Kitaev) and similarly $\eta\alpha=-1$ (AF Kitaev), forming an (η,α) parameter ring [10]. We will primarily focus on this idealized Hamiltonian but also consider some extensions such as farther neighbor couplings.

The phase diagram of H_{KH} on the honeycomb lattice is known from a combination of exact diagonalization [7,10], other numerical methods [11,12] and the presence of exactly soluble points. In addition to the exact solution using Majorana fermions of the Kitaev Hamiltonians $\alpha=\pm1$, and the obvious SU(2)-symmetric ferromagnet ($\eta=-1,\alpha=0$), a four sublattice site-dependent spin rotation [7] transforms H_{KH} at $\eta=+1,\alpha=1/2$ into a ferromagnet in the rotated basis. The original spins are then "stripy" ordered. Neel order from the Heisenberg antiferromagnet is unfrustrated on the bipartite honeycomb and was recently shown [10] to map under this transformation to a physical parameter regime hosting the spin pattern known as "zigzag."

This zigzag phase was determined in recent experiments [13–15] to be the low-temperature ordering pattern of Na_2IrO_3. The zigzag order was earlier theoretically found to be most stabilized by combining Kitaev interactions and the further neighbor [16,17] exchanges J_2, J_3, which naturally arise across a honeycomb hexagon [18,19] and which together fit the available experimental data in comparisons to exact diagonalization [20]. Indeed, within a classical approximation to the phase diagram (Luttinger-Tisza described below), the zigzag phase within the pure Kitaev-Heisenberg model lies nearly at the boundary of the large zigzag-ordered region stabilized by J_2,J_3 exchanges [21]. Interestingly, the zigzag phase in its $J_1-J_2-J_3$ limit and in its Eq. (1) limit may offer experimentally relevant distinguishing characteristics [10,22].

So far, only the honeycomb iridates Na_2IrO_3 and Li_2IrO_3 have been studied in the context of the Kitaev-Heisenberg model. Despite initial worries that trigonal distortion would invalidate the derivation of the Kitaev exchange discussed below, recent resonant inelastic x-ray scattering results [23]

support the validity of the strong spin-orbit coupling approach. For the sodium iridate Na_2IrO_3, attempts to extract the magnetic Hamiltonian from fits to experiments including susceptibility and spin wave spectra [10,13–15,20,24,25] and to electronic properties [22,26] have, so far, proved unable to distinguish between substantial Kitaev exchange and a complete lack of it. Few experimental results on magnetic behavior in the lithium iridate Li_2IrO_3 are currently available, though the relatively small magnitude of the Curie Weiss scale extracted from susceptibility suggests the Kitaev exchange may be strong [20,25].

Beyond the possible Kitaev-Heisenberg physics in the layered honeycomb iridates, other iridates have also attracted much attention. Layered compounds include the Mott insulator Sr_2IrO_4 [27,28] and its bilayer variant $Sr_3Ir_2O_7$ [29,30], both with ordered SOC magnetic moments. Notable examples with a fully three-dimensional structure include the 2-2-7 pyrochlore iridates, where changing the A site rare-earth metal yields radically varying properties [4,5,31,32]; the sodium iridate $Na_4Ir_3O_8$ spin liquid candidate, with Ir on the pyrochlore-descendent hyperkagome lattice [33]; and a recently epitaxially stabilized iridium spinel Ir_2O_4 with empty cation sites [34] leaving Ir on a pyrochlore lattice. Despite the variety of elemental composition and geometrical structure in this list, there is a simple but fundamental distinction separating the latter two compounds from the others listed.

In this manuscript, we show that the iridates $Na_4Ir_3O_8$ and Ir_2O_4, as well as possible compounds in certain other geometries, may be described by generalizations of the Hamiltonian (1) to the relevant lattices (hyperkagome for $Na_4Ir_3O_8$ and pyrochlore for Ir_2O_4). The key quantum chemistry ingredients, which can generate the interactions H_{KH}, have been already pointed out by Jackeli and Khaliullin [6] but the extension to three-dimensional lattices, as well as to these compounds, has not been previously exposed. We begin by recalling the derivation of H_{KH} and systematically extending it to other geometries in two and three dimensions; it applies when oxygen octahedra are edge-sharing, yielding lattices that are in a certain sense subsets of the fcc. We then proceed to investigate the phase diagram of H_{KH} on these lattices, using primarily analytical approaches. We generalize the honeycomb four-sublattice transformation into a duality on graphs and lattices with Kitaev labeled bonds in any dimension, and even with certain further neighbor pure Heisenberg couplings; we shall refer to it as the *Klein duality* since, as we shall show, it is structured by the Klein four-group $\cong\mathbb{Z}_2 \times \mathbb{Z}_2$. We give a simple algorithm determining which graphs admit the duality, based on this Klein group structure. The Klein duality gives stripy phases as FM duals. Diagonalizing the classical version of H_{KH} with spins of unconstrained length (i.e., the Luttinger-Tisza approximation), we identify unconventional ordering patterns and also find hints of quantum magnetically disordered phases, most interestingly on the hyperkagome. The Luttinger-Tisza phase diagrams are shown in Fig. 1. To directly capture Majorana fermion quantum spin liquids analogous to the Kitaev honeycomb QSL, we decompose spins into Majorana combinations of Schwinger fermions, a mean-field treatment, which is exact for the Kitaev honeycomb model, finding on all other lattices fermionic QSLs, which break time reversal and carry gapless excitations, but which are not exact solutions. For the honeycomb and hyperkagome pure Kitaev Hamiltonians, the lattice fragments under a bond type γ into disjointed localized clusters, giving flat bands in the Majorana mean field as well as in the Luttinger-Tisza approximation, which hints at a possible analogy between the honeycomb Kitaev QSL and the Kitaev Hamiltonian ground state on the hyperkagome.

We focus on two candidate materials, while also considering other related compounds. The recently epitaxially fabricated Ir_2O_4 is a spinel without the A cation, leaving the iridium ions on a pyrochlore lattice with oxygens positioned appropriately, as described below; Ir_2O_4 was found to be a narrow gap insulator [34]. The spin liquid candidate $Na_4Ir_3O_8$ is an iridate with $S = 1/2$ moments on the three-dimensional hyperkagome lattice, which exhibits no magnetic order down to at least 2 K [33]. In addition to these two iridates, this study may also capture compounds in which iridium is replaced by a transition metal ion with strong spin-orbit coupling, intermediate correlations and valency appropriate for a magnetic effective spin-1/2 model (see below). Recently, the osmium oxides $CaOs_2O_4$ and $SrOs_2O_4$ were computationally predicted [37] to be stabilized in the spinel structure relevant to Kitaev-Heisenberg physics; if they indeed exist in this geometry, H_{KH} should form at least part of their magnetic Hamiltonian. Kagome and triangular lattice iridates may be seen as appropriate layers within epitaxially stabilized Ir_2O_4, coupled together in a nontrivial manner. Triangular lattice iridates could potentially also be stabilized as analogues of the cobaltates [38] Na_xCoO_2, where Co is on a triangular lattice; the preferred valency would exist uniformly only in the limit $x \to 0$, but small x should offer interesting perturbations as well as likely separate layers of triangular lattices. However, no triangular lattice iridate with the relevant edge sharing octahedra structure is currently available; a compound of the type Na_xIrO_2 may or may not turn out to be stabilized.

In addition to the honeycomb Kitaev-Heisenberg model, other previous work has investigated Hamiltonians related to H_{KH} on other lattices. Chen and Balents [39] studied spin Hamiltonians on the hyperkagome lattice for $Na_4Ir_3O_8$, in the strong and weak SOC limits (relative to octahedral distortions). Within the strong SOC case, they considered the single superexchange pathway via oxygen ions generating the single point H_{KH} at $\alpha = 1/2$, for which they found that classical configurations of stripy patterns were completely unfrustrated [40] Superexchange via oxygen ions generating anisotropic spin interactions for the SOC Kramers doublet in $Na_4Ir_3O_8$ was also considered by Micklitz and Norman [41,42] in electronic structure computations and associated microscopic tight-binding parametrization. Recently, Reuther, Thomale, and Rachel [43] studied a family of related Hamiltonians including on triangular lattices formed by second neighbors of the honeycomb, with an associated hidden ferromagnet. Very recently, the classical H_{KH} Hamiltonian was studied on the triangular lattice by Rousochatzakis, Rossler, Brink, and Daghofer [44]. Their study included a classical Monte Carlo computation suggesting the intriguing possibility that Kitaev exchange can stabilize an incommensurate vortex lattice of the $\mathbb{Z}_2$ topological defects of the Heisenberg antiferromagnet 120° order.

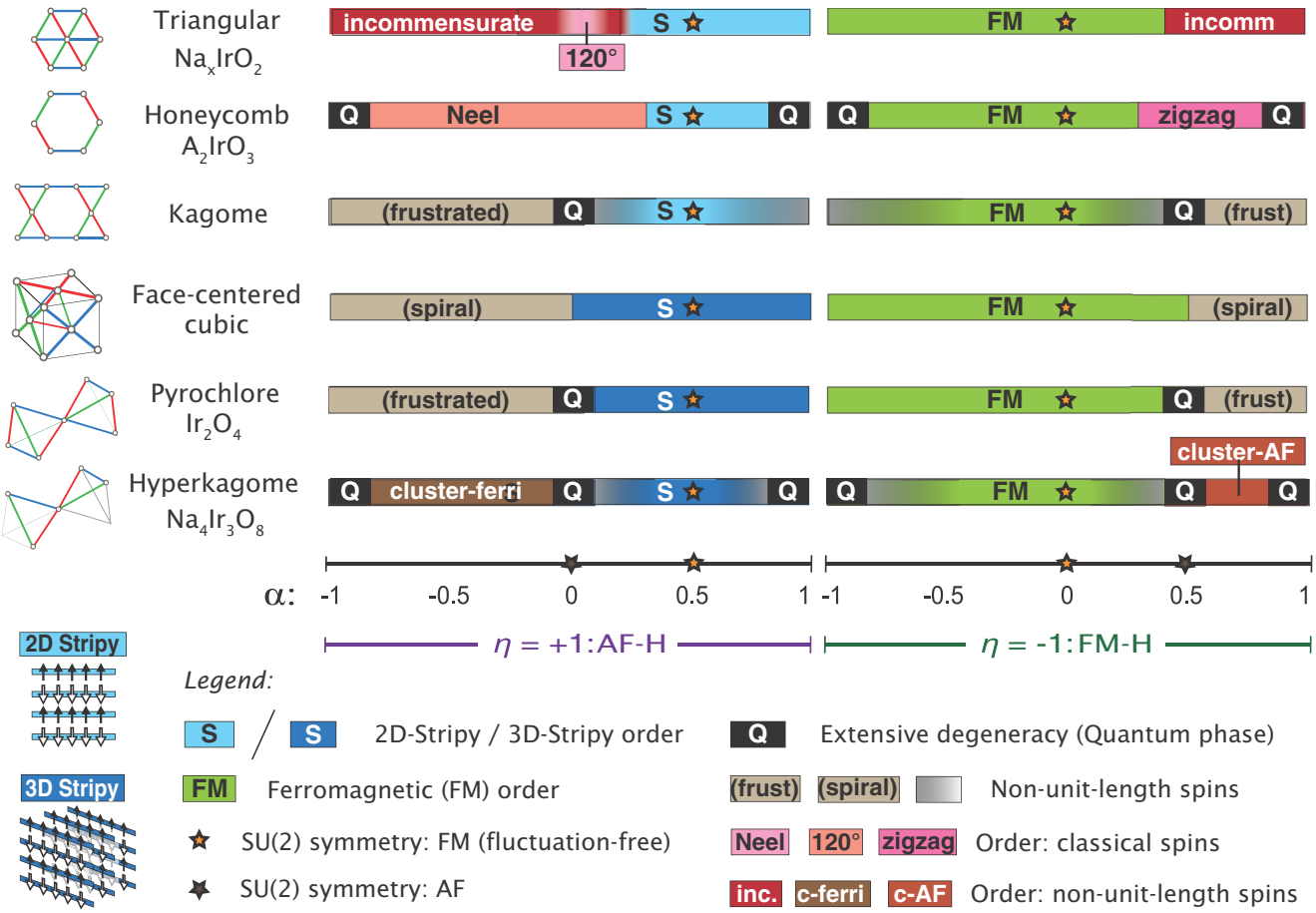

FIG. 1. (Color online) Phase diagrams using the Klein duality as well as the Luttinger-Tisza approximation (LTA). Phase diagrams are shown for the Kitaev-Heisenberg Hamiltonian, $H_{\rm KH} = \eta\,(1-|\alpha|)\,\vec{S}_i \cdot \vec{S}_j - 2\eta\alpha S_i^{\gamma_{ij}} S_j^{\gamma_{ij}}$ with $\eta = \pm 1$, on the various lattices. Note that the parameter space is a ring: for the α parameter segments shown here, the endpoints should be identified, i.e., writing the parameter as (η,α), identify the points $(-1,-1) \cong (+1,+1)$ and also identify the points $(-1,+1) \cong (+1,-1)$. Rich phase diagrams are found. 2D and 3D stripy magnetic phases (blue), found on all lattices, are exact and fluctuation-free by the Klein duality at the FM SU(2) point (yellow star) $\eta = +1$, $\alpha = 1/2$. On the kagome and hyperkagome lattices, outside the FM SU(2) points, the FM and stripy orders are given non-unit-length spins by the LTA (gray shading), suggesting frustration. Extensive degeneracy of LTA ordering wave vectors hints at a non-spin-ordered "quantum" phase, labeled "Q," where the Hamiltonians hosting Q phases have been solved, exactly [9] for the honeycomb at $\alpha = \pm 1$ and numerically [35,36] for the kagome at $\eta = +1$, $\alpha = 0$, they have turned out to host nonmagnetic phases. The hyperkagome hosts Q points at the Heisenberg antiferromagnet and its Klein dual, as well as at the pure Kitaev Hamiltonians, because any single Kitaev bond type fragments the hyperkagome into disjoint clusters (see Fig. 4). The 120° triangular lattice and Neel and zigzag honeycomb orders are found with normalized spins. Apparent ordering with LTA non-normalized spins is found at incommensurate wave vectors on the triangular lattice and in the cluster-ferrimagnet and cluster-antiferromagnet (AF) regimes on the hyperkagome. Kagome, fcc, and pyrochlore lattices also host frustrated regimes with no definitive ordering within the LTA, as described in the text (gray).

II. KITAEV COUPLINGS IN LATTICES BEYOND THE HONEYCOMB

Generating the Kitaev coupling requires a subtle recipe with ingredients from chemistry, geometry, and a hierarchy of energy scales, as we now recall [6,7,10]. Spin-orbit coupling is key, together with (intermediate) correlations; let us focus on iridium. The iridium ions should retain their $5d$ electrons in localized orbitals, and exist in the 4+ valence. Each iridium should be surrounded by six oxygen ions (or other electronegative ions with valence p orbitals), which form the vertices of an octahedron cage, shown in Fig. 2. The octahedral crystal field splits the $5d$ orbitals into an empty e_g pair and a triplet of t_{2g} orbitals with five electrons and one hole. Strong spin-orbit coupling further splits t_{2g} down to a half-filled Kramer's doublet, the spin-1/2 degree of freedom defining the low-energy manifold. The final key ingredient is the geometrical structure: edge sharing octahedra with 90° Ir-O-Ir bond angles.

In perturbation theory from the Mott insulator limit, virtual hopping of holes from iridium t_{2g} orbitals through intermediate oxygen p orbitals generate the low-energy spin Hamiltonian. There are multiple relevant exchange paths [7,10]. When holes hop through intermediate oxygens and meet on an iridium d orbital, the resulting coupling is a pure Kitaev term, and is proportional to $J_H/[(U_d - 3J_H)(U_d - J_H)] \approx J_H/U_d^2$. The iridium Coulomb exchange U_d and Hund's rule coupling J_H together specify all of the multiband interaction parameters, due to the symmetries of d orbitals. A second exchange path,

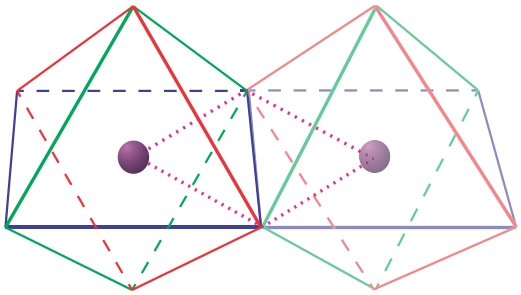

FIG. 2. (Color online) Edge-sharing IrO_6 octahedra generating Kitaev exchange. Iridium ions (spheres) are each coordinated by six oxygen ions forming vertices of octahedra. Octahedra of neighboring Ir ions share edges. Dotted (purple) lines show the iridium-oxygen-iridium hopping paths, which form a square with 90° angles. As described in the text, these superexchange paths generate an Ising interaction between the iridium effective spins, which couple a spin component x, y, or z depending on the orientation of the shared octahedra edge (shown in red, green, and blue). Ir lattices hosting this Kitaev exchange must arise from a regular tiling of these edge-sharing octahedra.

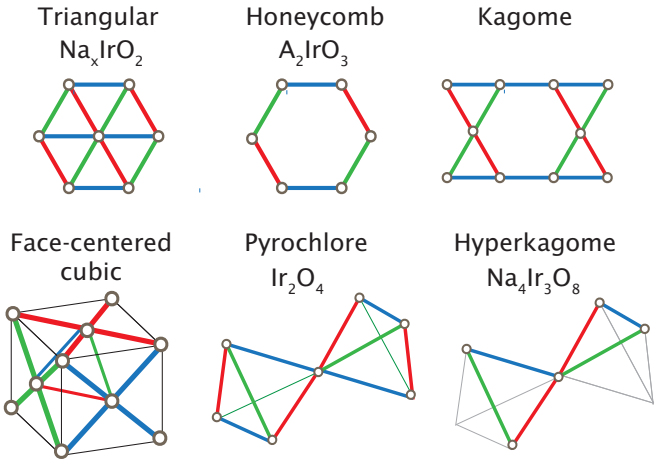

FIG. 3. (Color online) Kitaev-Heisenberg lattices. Iridium ions arranged in these lattices may generate the Kitaev spin exchange, coupling component x,y,z on bonds colored red, green, and blue, respectively. A blue colored bond connecting two Ir sites implies that the respective IrO^6 octahedra share a blue edge as in Fig. 2. We also list examples of possible relevant iridium compounds that form these lattices.

with two holes meeting on an oxygen or cycling around the Ir-O square, contributes a combination of Kitaev and Heisenberg couplings equal to $H_{\rm KH}$ at $\alpha = 1/2$, with a coefficient and sign η depending on the oxygen p orbitals charge-transfer gap and Coulomb repulsion. Direct iridium wave-function overlap gives a pure Heisenberg coupling. Recently [10], an additional pathway through the higher e_g orbitals has been proposed to be relevant as well, contributing $H_{\rm KH}$ at $\eta = -1$ and $\alpha = 1/2$. The interplay of these exchanges suggests α may not be computable microscopically.

Generalizing this derivation to geometries beyond the honeycomb requires preserving the edge sharing octahedra with 90° Ir-O-Ir bonds. Many commonly studied iridates such as the layered perovskites and the "2-2-7" pyrochlores have corner sharing octahedra and thus are not captured by this derivation. Figure 2 shows two adjacent octahedra, with edges color coded by the spin component coupling they generate when the octahedra of neighboring Ir ions share that edge. It is evident that all twelve octahedra edges may be shared while still maintaining 90° bonds and threefold symmetries (coupled space and spin rotations). Tiling octahedra, which touch along edges, builds a face-centered cubic (fcc) lattice of the octahedra centers.

We thus find that in two and three dimensions, all lattices whose graph of nearest-neighbor bonds is a subset of the nearest-neighbor bonds of the fcc, including the fcc itself, may host analogues of the Kitaev exchange. Possible geometries include the kagome and triangular lattices in two dimensions, and the face-centered cubic, pyrochlore (as realized in spinel-based compounds), and hyperkagome geometries in three dimensions. These are shown in Fig. 3. These six are commonly studied lattices which are such subsets of the fcc, but an infinite number of lattices may be added to this list. All the materials discussed above have these edge-sharing octahedral structures and their magnetic Ir ions form one of these lattices. As for the honeycomb iridates, reduced crystal symmetry distorting Ir-O angles away from 90° will generate other magnetic exchanges. Despite apparently strong >10% distortions of the bond angle in the sodium honeycomb iridate and a slew of experiments on this material, a Kitaev exchange comparable to or even stronger than the Heisenberg exchange is still consistent with current experimental results, suggesting a hopeful outlook for the other materials.

Note that the quantum chemistry considerations pictured in Fig. 2 tightly constrain the possible lattice realizations of Eq. (1). Specifically, these constraints are *tighter* than those imposed by naive symmetry considerations of SOC. For example, it is natural to define an implementation of SOC that couples spin component S^z to bonds along $\hat{z}$, i.e., locks the Bloch sphere to real space. This would generate Eq. (1) on the simple cubic lattice with S^zS^z coupling along $\hat{z}$ bonds, as well as on the square lattice with $\gamma = x,y$. However, the exchange pathways of Ir t_{2g} orbitals forbid this scenario. Instead, the analysis above shows that for t_{2g} orbitals, as in iridium, SOC couples the spin component S^z to the fcc lattice bonds lying normal to $\hat{z}$. The simple cubic lattice version of $H_{\rm KH}$ cannot be generated, and a compound structured as layers of a square lattice would collapse its Kitaev exchange to uniform Ising couplings along all square lattice bonds.

The honeycomb and hyperkagome lattices share a common feature distinguishing them from the other lattices: if we only keep bonds of a single Kitaev type γ, the lattice fragments into localized disconnected *clusters*. On the honeycomb, each cluster contains two sites, and forms the unit cell. On the hyperkagome, each cluster contains three sites, arranged into a line segment. For a given bond label γ, the twelve-site unit cell fragments into four disjointed clusters, whose line segments are oriented parallel within each of two pairs and perpendicular between the pairs. The structure on the hyperkagome unit cell is shown in Fig. 4. As discussed below, this fact has dramatic repercussions for the Kitaev Hamiltonians in both the Luttinger-Tisza approximation and

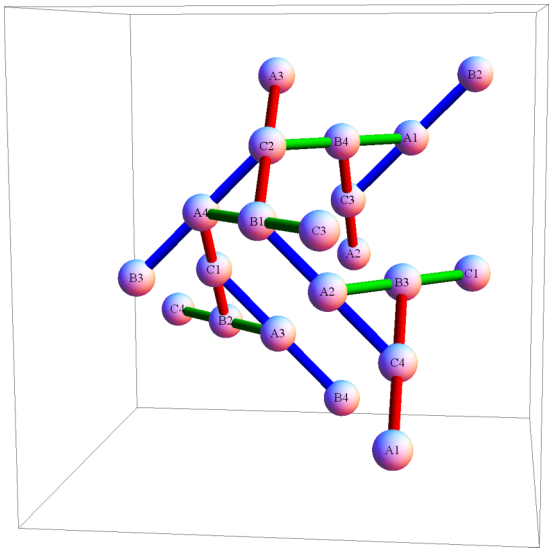

FIG. 4. (Color online) Hyperkagome unit cell and decomposition into Kitaev clusters. A symmetric depiction of the hyperkagome structure, highlighting the four disjointed three-site clusters, which split up the unit cell for a given Kitaev bond label (red, green, and blue). The fact that the lattice fragments into these disjointed clusters for a given Kitaev bond type has substantial repercussions, as described in the text. The four clusters of a given type appear in two parallel-orientation pairs that are perpendicular to each other (with different shading). The unit cell is composed of the 12 sites participating in the four drawn triangular faces, as well as all 24 drawn bonds. We label the 12 sites by a letter A, B, and C as in Ref. [45] so that A spins lie on midpoints of type-A (here blue) clusters, etc, and by a number 1–4 (chosen to not repeat within a triangle face or cluster). The camera angle, i.e., the vector pointing into the page, is just slightly off (up-right) of a Cartesian (here, also Bravais) axis; for $Na_4Ir_3O_8$, it is the vector from an iridium ion to a neighboring coordinating oxygen.

in the Schwinger fermion Majorana mean field (which on the honeycomb describes the Kitaev QSL). In both cases, certain excitations only propagate within a single Kitaev bond type γ, and the localized disconnected clusters imply these excitations must have completely flat bands.

III. KLEIN DUALITY AND HIDDEN FERROMAGNETS

A. Connections to previous work

Exactly solvable quantum Hamiltonians are rare in dimension higher than one. It is quite remarkable that the stripy phase at $\eta = +1$, $\alpha = 1/2$ found for the honeycomb Kitaev-Heisenberg model [7] is exact, a hidden ferromagnet exposed by the site-dependent spin rotation that quadruples the unit cell [46]. Unlike Neel order on even bipartite lattices, this stripy antiferromagnetic order is exact and fluctuation-free at $\alpha = 1/2$.

This "four-sublattice-rotation trick" has been known by Khaliullin and Okamoto for t_{2g} orbitals in a cubic environment since as early as 2002 [47]. It was used for Kitaev-Heisenberg-like Hamiltonians in ferromagnetic titanates [47,48] as well as in other systems, including an explicit transformation on the triangular lattice [49,50] to find the dual of 120° order for CoO_2. It was then applied to the honeycomb lattice by Chaloupka, Jackeli, and Khaliullin in their derivation of the Kitaev-Heisenberg model for the honeycomb iridates [7]. However, its general structure has not been previously elucidated. We will now show that this duality transformation may be defined on general graphs with Kitaev γ bond labels and that it has the structure of the Klein four-group, isomorphic to $\mathbb{Z}_2 \times \mathbb{Z}_2$. This will then lead to a geometrical condition specifying which lattices and finite graphs admit the Klein duality, a result especially useful for designing finite graphs for numerical studies.

B. Deriving the Klein transformation on graphs with Kitaev bond labels

We begin by defining a general unitary transformation, and then we will show that under certain special conditions it acts as a duality transformation on Eq. (1). Throughout this paper, by a "duality transformation" we refer to a mapping between Hamiltonians that maps a set of Hamiltonians (and the associated phase diagram) to itself (of course without mapping each particular Hamiltonian to itself). Consider a lattice or finite graph in any dimension that connects $S = 1/2$ spins, and assume each bond (i,j) carries a Kitaev *type* label

$$\gamma_{i,j} \in \{\mathbb{1}, x, y, z\}. \tag{2}$$

The set $\gamma \in \{x,y,z\}$ corresponds to Kitaev coupling $S_i^\gamma S_j^\gamma$ on that bond, where $\{x,y,z\}$ identifies a set of orthogonal axes in the spin Bloch sphere. The Hamiltonian on the bond may have other terms such as Heisenberg coupling and various anisotropies; but the transformation will turn out to be most useful if the coupling includes only Kitaev and Heisenberg terms, as in Eq. (1). The label $\gamma_{i,j} = \mathbb{1}$ can be assigned to a bond that does not have a Kitaev exchange (only Heisenberg and possible anisotropies), such as a second- or third-neighbor interaction. In general, such farther neighbor interactions supplementing $H_{\rm KH}$ will frustrate the transformation, so when making use of the Klein duality, the lattice should usually be considered to be just the pure nearest-neighbor Kitaev-Heisenberg model $H_{\rm KH}$, where all bonds carry $\gamma \in \{x,y,z\}$. However, we will show below that certain farther neighbor Heisenberg interactions do preserve the duality structure, and may be fruitfully included as $\gamma = \mathbb{1}$.

Let us proceed by describing the relevant transformations on individual sites. Assign each site a label

$$a_i \in \{\mathbb{1}, X, Y, Z\}, \tag{3}$$

which will specify a unitary transformation on that site, specifically rotation by π around the Bloch sphere axis S^a for $a \in \{X,Y,Z\}$, and no rotation for the identity element $a = \mathbb{1}$. Note that π rotation around S^a flips the sign of the spin components perpendicular to a, so that the rotation $a_i = Z$ multiplies the (x,y,z) components of S_i by the sign structure $g[Z] = (-1,-1,1)$, and also that $g[\mathbb{1}] = (1,1,1)$.

Now, observe that both bond labels $\gamma_{i,j}$ and site labels a_i may be interpreted as elements of the single set $\{\mathbb{1}, X, Y, Z\}$. We may turn this set into a group by defining a multiplication rule. A possible definition is suggested by the multiplication

of the associated sign structures g, which entails, for example, $g[X]g[Y] = g[Z]$, suggesting we should define $XY = Z$. The resulting multiplication table is defined by

$$X^2 = Y^2 = Z^2 = XYZ = \mathbb{1} \tag{4}$$

with $\mathbb{1}$ acting as the identity. This is the presentation of the group with generators (X,Y,Z) and relations (X^2, Y^2, Z^2, XYZ), known as the *Klein four-group*. The Klein group is Abelian and with four elements is the smallest noncyclic group; it is isomorphic to $\mathbb{Z}_2 \times \mathbb{Z}_2$.

There is an alternative, *geometrical,* way to define multiplication on the elements a_i and $\gamma_{i,j}$. We define the geometric multiplication $(*)$ of a site i and one of its bonds (i,j) to be the site reached by traversing the bond, $i * (i,j) = j$. The associated Klein group elements a_i and $\gamma_{i,j}$ inherit this geometric multiplication as

$$a_i * \gamma_{i,j} = a_j. \tag{5}$$

The Klein group product $(\times)$ and the geometric multiplication $(*)$ are consistent on a bond if they give the same answer, $a_i * \gamma_{i,j} = a_i \times \gamma_{i,j}$. We say the transformation given by site labels $\{a_i\}$ is the *Klein* transformation if the geometrical multiplication is consistent with Klein group multiplication on *every* bond in the lattice.

If the transformation site labels a_i, a_j across a bond are consistent with the Klein group product, i.e.,

$$a_i \times \gamma_{i,j} = a_j, \tag{6}$$

or equivalently, (since elements in the Klein group square to the identity)

$$a_i \times a_j = \gamma_{i,j}\ , \tag{7}$$

then the transformation changes the form of a Kitaev-Heisenberg coupling in an especially simple way. This is simply because the sign flips $g[a]$ multiply by the Klein group rules, so the diagonal spin exchange $\sum_\alpha J^\alpha_{i,j} S^\alpha_i S^\alpha_j$ transforms by

$$J^\alpha_{i,j} \to g[a_i]_\alpha g[a_j]_\alpha J^\alpha_{i,j} = g[\gamma_{i,j}]_\alpha J^\alpha_{i,j}, \tag{8}$$

where $g[a]_\alpha \in \pm 1$ is component number α of the vector $g[a]$ of ± 1 signs. The transformation flips the sign of the components of J perpendicular to the bond type label. For Kitaev Heisenberg exchange, this means that the Heisenberg coefficient flips sign and the Kitaev coefficient gains twice the (old) Heisenberg coefficient.

Even if the transformation labels on two sites are consistent with the Klein group product on that bond, it might seem improbable that the a_i rotation labels can be chosen across the entire lattice in a pattern that is Klein group consistent on all bonds. Such consistency for all bonds is necessary for the transformation to change the Hamiltonian uniformly. Now, the Klein group structure shows its worth. The condition on the transformation $\{a_i\}$—consistency between geometric and Klein group multiplication on each bond—can be expressed as a condition that refers only to the lattice: that the $\gamma_{i,j}$ encountered in any closed path multiply to the identity $\mathbb{1}$. In other words, all closed loops on the lattice must be composed of the identity operators $\mathbb{1}, X^2, Y^2, Z^2, XYZ$. Then the transformation may be consistently defined by Klein group multiplication of bond labels on a any path,

$$a_j = \left(\prod_{\ell \in \text{path}_{i\to j}} \gamma_\ell \right) a_i. \tag{9}$$

C. Geometrical condition for the Klein duality

We have shown that the existence of the Klein duality can be expressed as a condition on the lattice. Using the Klein group structure, we can write this condition as follows. *Any closed loop, containing N_x x, N_y y, and N_z z bonds, must satisfy*

$$N_x,\ N_y, \text{ and } N_z \quad \text{all even or all odd.} \tag{10}$$

The three N_i' s can be all even because Klein group elements square to the identity, or all odd because $XYZ = 1$. If this condition, Eq. (10), is satisfied on all closed loops then the Klein duality can be constructed consistently as follows: choosing a reference site i, which for simplicity will be unchanged in the duality, $a_i = \mathbb{1}$, assign any site j a rotation label a_j as simply the Klein group product of the Kitaev bond labels γ on any path from i to j. The constraint (10) ensures this duality construction is consistent regardless of the choice of paths i to j. The Klein duality then maps Eq. (1) to itself, transforming the parameters α and η according to Fig. 5.

It is easy to see that the Klein duality indeed exists on all of the infinite lattices shown in Fig. 3; because the Klein group is Abelian, it is sufficient to check that the condition is satisfied on small local loops. For example, triangle faces have $N_x = N_y = N_z = 1$. The condition also holds on other lattices such as the simple cubic that can host symmetric Kitaev exchange but cannot generate it via t_{2g}-p orbital superexchange. Adding pure Heisenberg ($\gamma = \mathbb{1}$) further neighbor interactions generally spoils the Klein duality, though if all the resulting loops satisfy Eq. (10), the Klein duality survives unscathed and, moreover, does not modify the pure Heisenberg $\gamma = \mathbb{1}$ interactions, even while it flips the sign of Heisenberg interactions on Kitaev-labeled bonds. This occurs, for example, with J_3 Heisenberg exchanges on the honeycomb and kagome lattices, connecting sites on opposite corners of a hexagon. The family of Hamiltonians preserved by the duality is then enlarged to $J_K - J_1 - J_3$, i.e., nearest-neighbor Kitaev-Heisenberg plus third-neighbor Heisenberg. This $J_K - J_1 - J_3$ family of Hamiltonians maps to itself (nontrivially) under the Klein transformation, with J_3 unchanged.

For graphs and finite lattices with periodic boundary conditions (PBC), considering small local loops is insufficient; loops traversing the PBC may break Eq. (10) and spoil the Kitaev duality. Such winding loops must be checked explicitly. Here condition (10) should serve much practical use, as finite-sized versions of the Fig. 3 lattices with PBC are useful for numerical studies, and it may otherwise be difficult to construct or identify the choice of PBC that admit the Klein duality. In many cases, the appropriate PBC involve nontrivial twists that, in a continuum limit, appear as cutting and gluing operations on the boundaries.

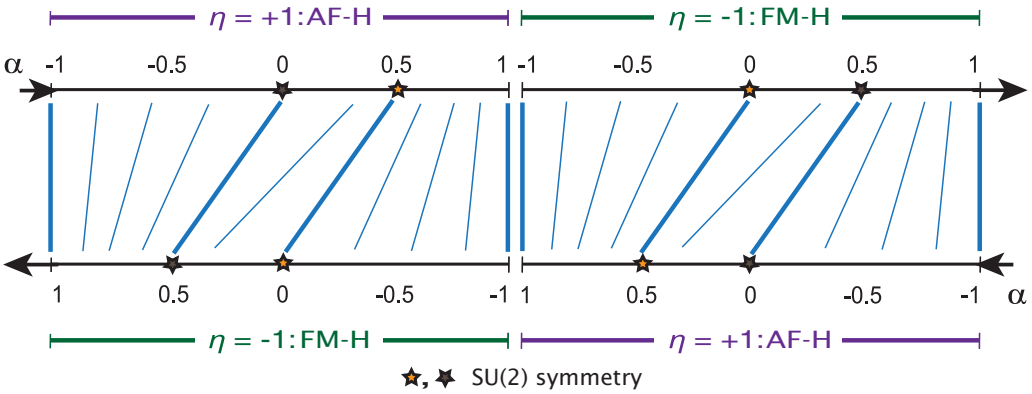

FIG. 5. (Color online) Action of the Klein duality on the Kitaev-Heisenberg Hamiltonian. The η,α parameters on the top line (oriented left to right) of the Hamiltonian (1) map according to the blue lines to η,α parameters on the bottom line (oriented right to left) in the Klein-dual Hamiltonian. Thick blue lines map the points shown exactly, thin blue lines are a qualitative sketch. Note that the right and left edges of the figure are identified, forming a ring. Both pure Kitaev Hamiltonians ($\alpha = \pm 1$) are *self-dual*, mapping to themselves. The points at $\alpha = 1/2$ and $\eta = +1$, $\eta = -1$ are dual to the SU(2) symmetric FM-Heisenberg and AF-Heisenberg points (yellow and brown stars), respectively, with the FM dual point hosting the exactly soluble *stripy* phases on all lattices in Fig. 3.

D. The Klein duality on H_{KH}, Klein self-dual points, and Klein $\mathbb{Z}_2$ symmetry

In order to describe the action of the Klein duality on the parameter space of Eq. (1), let us first discuss the η,α, and other parametrizations. In Eq. (1), the sign $\eta = \pm 1$ is the sign of the Heisenberg exchange and the sign of α is minus the relative sign between the Kitaev and Heisenberg exchanges. This is a compatible extension of the α parametrization introduced in Ref. [7]; restricting to $\eta = +1$, $0 \leqslant \alpha \leqslant 1$ gives the original parameter space [7] with antiferromagnetic (AF) Heisenberg and ferromagnetic (FM) Kitaev interactions. It is clear that both the FM and AF pure Kitaev Hamiltonians are each described by two parameter points, which must be identified,

$$\begin{aligned}(\eta = +1, \alpha = +1) &\cong (\eta = -1, \alpha = -1),\\ (\eta = +1, \alpha = -1) &\cong (\eta = -1, \alpha = +1).\end{aligned} \tag{11}$$

Identifying (i.e., gluing) these pairs makes the (η,α) parameter space into a circle. In the axis shown at the top of Fig. 5, the two α segments (for $\eta = +1, -1$) are connected both in the middle where they are drawn to almost touch and also at their distant endpoints (where arrows are drawn). Comparing to the angular parametrization presented in Ref. [10], $\eta = +1 (\eta = -1)$ is the right(left) side of the circle, and $\alpha = -1, \ldots, +1, -1, \ldots, +1$ increases going clockwise. (We will also sometimes refer to both FM and AF pure Kitaev Hamiltonians simultaneously, in which case the notation $\alpha = \pm 1$ is unambiguous.) Note that the η,α parametrization, though (piecewise) linear, is nonanalytic at $\alpha = 0, \pm 1$, which may be an issue for certain numerical computations.

Now we may discuss how the Klein duality acts on Eq. (1). In other words, the Hamiltonian (1) with certain parameters η,α is equivalent to the Hamiltonian (1) on the rotated spins but with different parameters η',α'. The duality is shown by the blue lines in Fig. 5. Note that where the blue lines are roughly vertical, the duality approximately just flips the sign of both η and α, i.e., just flips the sign of the Heisenberg term. In general, it flips the sign of the Heisenberg term but also adds twice the (old) Heisenberg term to the Kitaev term,

$$\begin{aligned}&J_H \vec{S}_i \cdot \vec{S}_j + J_K S_i^{\gamma_{ij}} S_j^{\gamma_{ij}}\\ &\quad\longrightarrow (-J_H)\vec{S}_i \cdot \vec{S}_j + (J_K + 2J_H) S_i^{\gamma_{ij}} S_j^{\gamma_{ij}}.\end{aligned} \tag{12}$$

Note that with Eq. (1) as written, changing α also changes the overall energy scale; this can be avoided by dividing Eq. (1) by $(1 - |\alpha|)$, so that the magnitude of the Heisenberg term remains fixed at 1.

On Eq. (1), the duality always takes $\eta \to -\eta$, but acts on α in a nonlinear way, approximately shown by the changing slope of the blue lines in Fig. 5. The relation between α and α' is given implicitly by

$$\alpha'\alpha = (1 - c_{\alpha'})(1 - c_\alpha), \quad c_\alpha \equiv \begin{cases} 0, & \alpha \leqslant 0 \\ 2\alpha, & \alpha \geqslant 0 \end{cases}. \tag{13}$$

As is clear from Fig. 5, the relation may be written explicitly as a simple piecewise function,

$$\alpha' = \begin{cases} \frac{1}{\alpha+2}, & -1 \leqslant \alpha \leqslant 0 \\ \frac{1-2\alpha}{2-3\alpha}, & 0 \leqslant \alpha \leqslant \frac{1}{2} \\ \frac{1}{\alpha} - 2, & \frac{1}{2} \leqslant \alpha \leqslant 1 \end{cases}. \tag{14}$$

The family of Hamiltonians (1) can be generalized by modulating the strength of couplings on different bonds in arbitrary ways; the Klein rotation generalizes as well to arbitrary configurations of coupling strengths. Generically, it will no longer map one simple family of Hamiltonians to itself, but it may still offer hidden exactly solvable points, such as by mapping Eq. (1) with toric code anisotropies of the Kitaev coupling strength into a mixed Ising-Heisenberg ferromagnet with an exact ground state. Specifically, given Kitaev bond strengths of $(1 - a/2, 1 - a/2, 1 + a)$ on the three bond types, the location of the hidden Ising ferromagnet shifts to $\eta = +1$, $\alpha = 1/(2 - a/2)$.

Duality relations in condensed matter physics typically map order to disorder or strong coupling to weak coupling, such as the duality relating the paramagnetic and ferromagnetic phases in the transverse field (quantum) Ising model. The

Klein rotation is a duality in the sense of mapping a family of Hamiltonians to itself, but it is not amenable to this typical interpretation. First, there is no sense of weak and strong coupling regimes within the parameter space of Eq. (1). Second, this parameter space forms a ring, and rather than a single self-dual point, it offers *two* distinct Hamiltonians, which are self-dual under the Klein duality. Third, as is rigorously known for the honeycomb lattice and suggested by the LTA for the other lattices below, the self-dual pure Kitaev Hamiltonians lie in the interior of a phase rather than signifying a phase boundary.

The Hamiltonians at the two Klein self-dual points may alternatively be interpreted as possessing an enlarged symmetry group. The additional symmetry is generated by the Klein duality and has $\mathbb{Z}_2$ characteristic. It thus acts in a highly nontrivial manner on spins on different sites. Phases that preserve this Klein $\mathbb{Z}_2$ symmetry must contain this highly nontrivial structure; there is currently one known example of such a phase, the Kitaev honeycomb spin liquid. If any lattice turns out to host a magnetically ordered phase, which does not spontaneously break the Klein $\mathbb{Z}_2$ symmetry, such a phase would have a complex pattern of noncoplanar spin order. This is unlikely, but there may also be phases that break the Klein $\mathbb{Z}_2$ symmetry but do not break too many other symmetries, yielding a ground-state manifold that naturally splits into the two Klein $\mathbb{Z}_2$ broken portions. Determining which or whether any of these scenarios holds on any particular lattice is left for future work.

IV. EXACTLY SOLUBLE STRIPY PHASES AS KLEIN DUALS OF THE FERROMAGNET

The most obvious consequence of the existence of the Klein duality is seen by applying the duality on the Heisenberg ferromagnet. At the resulting parameter point $\eta = +1, \alpha = 1/2$, the ground-state manifold of the quantum Hamiltonian is known exactly and consists of simple product states, parametrized by the full SU(2) symmetry. The ground states may be found by taking a ground state of the Heisenberg ferromagnet and applying the rotations defined by the Klein duality on this magnetic order. The result is the *stripy* collinear magnetic order. We will use the name *stripy* to refer to the FM-dual phase on lattices in any dimension, both to preserve the analogy to the honeycomb and also because, as shown below, the 3D-stripy orders can have some "stripy" features in their own right.

Away from the SU(2) symmetric point, the symmetries reduce to the lattice SOC operations. The stripy ordering breaks the threefold rotation symmetry, present in all Kitaev lattices as in Fig. 3, that simultaneously permutes the suitably chosen Euclidean directions $\hat{x} \to \hat{y} \to \hat{z} \to \hat{x}$, the same axes on the Bloch sphere and also the Kitaev bond labels $x \to y \to z \to x$. The appropriate coordinate system is set by an IrO_6 octahedron, in which the ordering is along one of the three directions $(1,0,0),(0,1,0),(0,0,1)$, i.e., $\hat{x},\hat{y},\hat{z}$. $\hat{z}$-type stripy order has z-bonded spins aligned parallel and x or y bonded spins aligned antiparallel. The collinear spin axis is then fixed to S^z, though the direction of the ordered moment will likely be determined by other effects in any material realization.

The stripy orders on the various lattices share common features but also host distinguishing characteristics. On the two-dimensional lattices, which always appear as layers perpendicular to the $(1,1,1)$ axis in the IrO_6 coordinate system, the ordering breaks the (SOC version of) 120° lattice rotation symmetry. On the triangular lattice, it is literally alternating stripes (i.e., lines of sites) of up spins and down spins. On the honeycomb lattice, each stripe is composed of the two-site clusters that lie on a given line; this order is also known as "IV" in the J_1-J_2-J_3 literature. On the kagome lattice, stripy order gives the same configuration on each unit cell (is wave vector Γ) of two spins up and one spin down, meaning it is *ferrimagnetic* with a nonzero net magnetization. At the exact $\alpha = 1/2$ point, the spins are saturated and the net magnetization is $1/3$ that of the ferromagnet.

In three dimensions, the 3D-stripy orders involves alternating planes of up spins and down spins. For say $\hat{z}$ stripy order, the planes are normal to $\hat{z}$. On the fcc lattice, the planes are faces of the fcc cube. On the pyrochlore lattice, the stripy order acquires an additional feature: spin-up planes are broken up into *chains* aligned in one particular direction, and spin-down planes are composed of chains aligned in the perpendicular direction. On the hyperkagome lattice, this feature persists, and, moreover, the chains are broken into oriented linear clusters: for z-stripy order, the z-type three-spin-chain clusters of Fig. 4 are oriented uniformly within the spin-up planes, and also uniformly but in a perpendicular orientation within the spin-down planes. The 3D-stripy orders are shown in Fig. 6.

V. LUTTINGER-TISZA APPROXIMATION PHASE DIAGRAMS

Except for the Heisenberg ferromagnet and its Klein dual point as described above, the Kitaev-Heisenberg Hamiltonians are *frustrated* [51]. The resulting sign problem for quantum Monte Carlo renders their quantum phase diagrams, especially for the three-dimensional lattices, exceedingly difficult to compute. The Hamiltonians (1) on the various lattices are quite unique in that they all offer an exact solution at a nontrivial point in the phase diagram, the Klein dual to the ferromagnet. To explore the remainder of the phase diagrams, we must use approximation methods, as we shall now describe.

For an initial survey of the phase diagrams, we employ the Luttinger-Tisza approximation (LTA), also known as the spherical model [52–55]. It is a semiclassical approximation in that it improves upon the classical Hamiltonian, incorporating some notion of quantum fluctuations and a reduced ordered moment. While the classical version of a Hamiltonian has the hard constraint that the ordered moment (i.e., the spin vector) on each site must have magnitude S, quantum fluctuations are expected to relax this constraint. Implementing this constraint only on average with a single global Lagrange multiplier, the Hamiltonian (1) becomes free quadratic and the lowest-energy configuration of the classical spins may simply be found by a Fourier transform and a diagonalization of the spin and sublattice indices.

The LTA always computes a lower bound to the energy of the *classical* model; this inequality becomes a strict equality when the LTA minimum energy configuration happens to obey the unit length constraint. In turn, classical configurations of spins with length S give upper bounds to the true ground-state energy of a spin-S quantum Hamiltonian [56], simply by

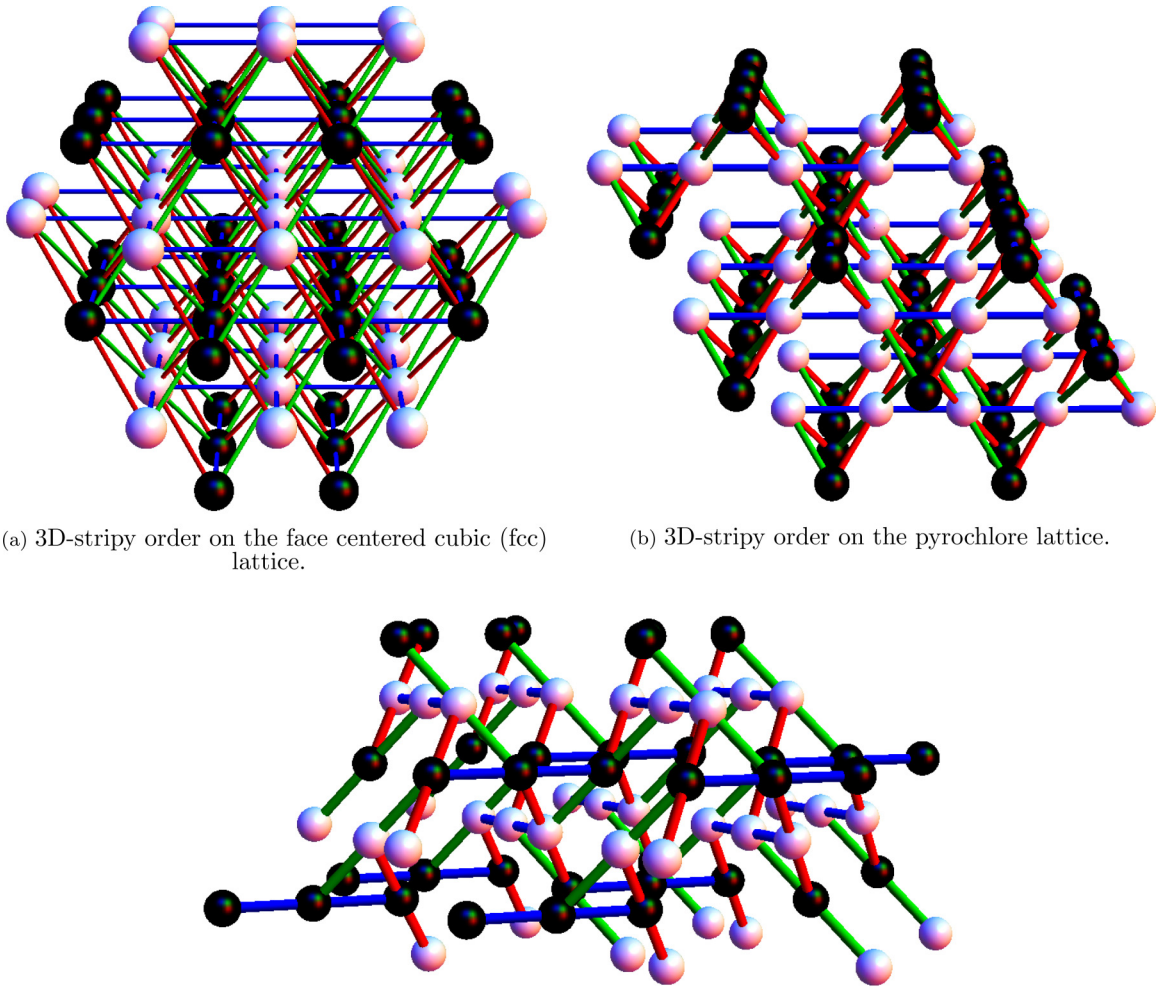

(a) 3D-stripy order on the face centered cubic (fcc) lattice.

(b) 3D-stripy order on the pyrochlore lattice.

(c) 3D-stripy order on the hyperkagome lattice.

FIG. 6. (Color online) 3D-stripy orders on the fcc, pyrochlore, and hyperkagome lattices. Black (white) spheres represent up (down) spins. Bonds are colored red, green, and blue according to the Kitaev label. The ordering pattern is of alternating planes, here normal to $\hat{z}$; z-type bonds (blue), i.e., those within the planes, connect spins of the same orientation. On the pyrochlore and hyperkagome lattices, planes are broken up into uniformly oriented chains, with chains in spin-up planes oriented perpendicularly to chains on spin-down planes. On the hyperkagome lattice, the chains are further broken into the linear three site clusters shown in Fig. 4. These stripy orders are exact at $\eta = +1, \alpha = 1/2$, being Klein duals of the ferromagnet.

defining site-product wave functions, which by the variational principle have at least the ground-state energy. When a non-normalized configuration is chosen by the LTA, its energy is lower than the classical minimum energy, which, in turn, is generally higher than the quantum ground-state energy, so the energy of the LTA configuration can match the true ground-state energy. Relaxing the unit length constraint, indeed, allows the classical ordered moments to fluctuate, and in some ways improves upon the constrained classical Hamiltonian as an approximation to the quantum Hamiltonian.

On a Bravais lattice and for the case with SU(2) spin rotation symmetry, solutions with normalized spins can always be constructed from the LTA minimum eigenvalues [55]. For momenta q satisfying $q = -q$, there is a family of degenerate orders but even for arbitrary incommensurate momenta, there are coplanar spiral solutions with normalized spins, with the first(second) spin component modulated by the real(imaginary) part of $\exp(iqr)$. However, when SU(2) spin rotation symmetry is broken such as by SOC, there may only be one low-energy spin component and this approach can fail, requiring $q = -q$ to construct states with unit length normalized spins. On lattices with multiple sites per unit cell, the LTA may assign different lengths to sites in the unit cell, which again points to frustration, though if the spins have nearly the same length, we expect the ordering pattern to be robust [57]. Note that even when classical solutions do exist, when the LTA identifies extensive ground-state degeneracy or includes degenerate ground-state configurations with vanishing ordered moment, it suggests quantum fluctuations will melt any magnetic order. In such cases, determining the ground state requires a full quantum analysis. Thus while the Luttinger-Tisza approximation cannot characterize nonclassical phases, it is a useful first approach for identifying features in the phase diagram.

The LTA phase diagrams are shown in Fig. 1. Here, we discuss general features; see Ref. [58] for details. Stripy phases

are found surrounding the FM-dual point in all of the lattices; they are exact ground states at $\eta = +1, \alpha = 1/2$ even within the LTA. However, the kagome and hyperkagome lattices exhibit an interesting frustration: while spins are uniformly normalized at the SU(2) FM-dual point, away from $\alpha = 1/2$ the energy is minimized when spins within the unit cell are of different lengths. As it must by the Klein duality, this frustration is observed in the ferromagnet phase as well. Evidently, for the kagome and hyperkagome, but not for the pyrochlore or the other lattices, even small SU(2) breaking within the ferromagnetic phase creates substantial frustration visible in the LTA.

At certain points in the phase diagram, all wave vectors in the BZ offer spin configurations with the same minimum energy, so that the lowest band is flat. While subextensive degeneracies occur generically at certain parameter points and are expected to be completely lifted by boundary conditions, such extensive degeneracies, marked by "Q" in Fig. 1, likely signify a new phase. What could the new phase be? There are only two Hamiltonians hosting LTA extensive degeneracies for which the quantum ground state is known: the honeycomb Kitaev model ($\alpha = \pm 1$), which is exactly soluble, hosting the Kitaev QSL with Majorana fermionic spinons; and the kagome Heisenberg antiferromagnet, which was recently found by DMRG simulations [35,36] to host a QSL phase, consistent with a bosonic $\mathbb{Z}_2$ QSL [59]. The ground states of pyrochlore and hyperkagome Heisenberg antiferromagnets, which also have LTA flat bands, are not conclusively known but have been proposed to be plaquette or dimer valence bond solids (VBS) as well as various fractionalized QSLs [60–63].

There are thus two conclusions to draw about the other Q points in Fig. 1. First, by the Klein duality, any lattice hosting a phase with no magnetic order in its AF Heisenberg model also has the same type of phase surrounding the $\eta = -1, \alpha = 1/2$ point, with FM Heisenberg and AF Kitaev exchanges. For example, the recent discovery of the kagome AF Heisenberg QSL then immediately yields the Klein dual of this QSL at the dual point; this Klein dual QSL will likely have distinct physical properties in its response to external fields. Second, by analogy with the known Q points mentioned above, we may guess that the pure Kitaev models on the hyperkagome also host a quantum phase with no magnetic order, either a VBS or a QSL.

It is especially encouraging that the LTA flat bands within the honeycomb and the hyperkagome pure Kitaev models arise via the same mechanism. Consider that LTA flat bands in the AF Heisenberg models occur due to the lattice specific band structure from a hopping model with π flux. For the pure Kitaev models $\alpha = \pm 1$, a given spin component such as S^z hops only on z-type bonds. As mentioned above, for the honeycomb and hyperkagome lattices, turning off y and x bonds splits the lattice into an extensive number of localized disconnected segments, as shown for the hyperkagome in Fig. 4. Localization in the disjointed clusters yields the flat bands. Moreover, unlike for the Heisenberg case, where (in the relevant lattices we study) there are gapless excitations when the flat lowest band touches higher ones, for the Kitaev cases, the disjointed clusters yield a band structure where all bands are completely flat and fully gapped, and in the hyperkagome case also fourfold degenerate at each wave vector due to four clusters in the unit cell.

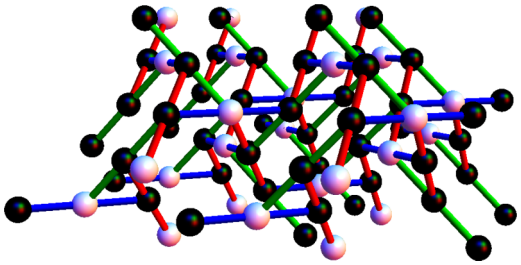

FIG. 7. (Color online) Magentic order of the cluster-ferrimagnet state on the hyperkagome. Black (white) spheres are up (down) spins; bonds are colored according to Kitaev label. Here shown for $\hat{z}$ ordering, notice that the z-type clusters (blue), lying in planes normal to $\hat{z}$, all have (up, down, up) spin configurations. This configuration has *nonzero* net magnetization. Note that the cluster-ferrimagnet order is Klein dual to the cluster-AF order.

Returning to the survey of the LTA phase diagrams, we find other regions with strong frustrations. On the kagome and pyrochlore lattices, over wide regions of parameter space, the LTA fails spectacularly: in the regimes labeled "frustrated," the unit cell in both lattices has two spins aligned antiparallel but with the remaining one (kagome) or two (pyrochlore) spins chosen to have exactly zero ordered moment by the LTA. Viewing the LTA as an enhancement of classical solutions, which incorporates quantum fluctuations, we see that here the expected quantum fluctuations are sufficiently strong to eliminate some of the ordered moments, pointing to especially strong quantum frustration. A related regime on the fcc lattice, a Bravais lattice, finds subextensive degeneracy involving incommensurate momenta, which would form spiral orders but with only one low-energy spin component cannot achieve correctly normalized spins across the spiral.

Finally, on the hyperkagome lattice, the LTA finds two regimes with apparent magnetic order with unconventional spin configurations. Though, in both cases, the spins crossing the unit cell are not chosen to have the same ordered moment; this is expected with such a large unit cell, and the LTA configurations should serve as good starting points for quantum Hamiltonian ground states, likely with quantum fluctuations greatly reducing the ordered moment. For $\eta = +1$ and $\alpha < 0$, we find that for z-type order, z clusters all have the identical spin ordering "(up, down, up)," resulting in an AF state with a nonzero net magnetization, which we thus term the "cluster ferrimagnet." The Klein dual of this order, for large α at $\eta = -1$, has the same "(up, down, up)" pattern in each z cluster except clusters are flipped on alternating planes, so there is zero net magnetization; we term it the "cluster-AF" state. These two Klein dual orders are shown in Figs. 7 and 8.

VI. SEARCHING FOR ANALOGUES OF THE KITAEV MAJORANA SPIN LIQUID BEYOND THE HONEYCOMB

All the lattices in Fig. 3, except the honeycomb, have coordination number larger than three, spoiling the Kitaev honeycomb spin liquid exact solution. However, similar Majorana QSL phases could still occur for the Kitaev Hamiltonians on the other lattices, only without an exact solution and with nonzero correlation length. Since it is generally highly

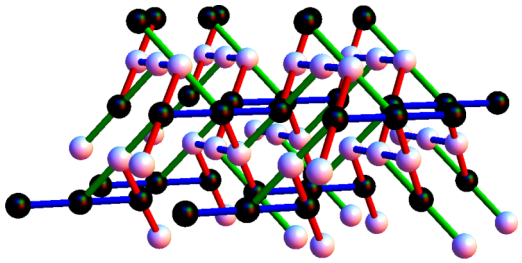

FIG. 8. (Color online) Magentic order of the cluster-AF state on the hyperkagome lattice. Black (white) spheres are up (down) spins; bonds are colored according to Kitaev label. Here shown for $\hat{z}$ ordering, notice that the z-type clusters (blue), lying in planes normal to $\hat{z}$, have (up, down, up) spin configurations on even-numbered planes, and the opposite (down, up, down) spin configurations on odd-numbered planes. This configuration has *zero* net magnetization. Note that the cluster-AF order is Klein dual to the cluster-ferrimagnet order.

difficult to determine whether the true ground state of a spin Hamiltonian forms a QSL, we will not attempt to answer this question. Instead, we will study possibilities for similar Majorana QSLs on the other lattices using an appropriate choice of mean field.

The exact solution of the Kitaev honeycomb model in terms of Majorana fermion operators is a specific case of a Schwinger fermion decomposition mean field, which becomes *exact* for this model [64–66]. To search for similar Majorana QSLs on the other lattices, we thus employ this mean field. Spins are decomposed into bilinears in four Majorana species $\chi^{0,1,2,3}$ as

$$S^a \to i\chi^0\chi^a \quad \text{with} \quad \{\chi^a,\chi^b\} = \delta^{a,b}. \tag{15}$$

This mapping is exact under the single fermion occupancy constraint $\chi_i^0\chi_i^1\chi_i^2\chi_i^3 = 1/4$. On the honeycomb lattice, this constraint commutes with the pure Kitaev Hamiltonian, but that does not occur on the other lattices. The $\mathbb{Z}_2$ gauge freedom in defining the Majorana operators enables a choice of attaching gauge transformations to the physical symmetry operations, called a projective symmetry group (PSG) [67]; see Ref. [58] for details. The PSG of the Kitaev honeycomb model was previously studied [64] and determined to be flux-free, with (χ_1,χ_2,χ_3) transforming as a pseudovector and each bond permitting Majorana bilinear expectation values only for two Majoranas of the same species a, yielding a total of three mean-field parameters:

$$u_\gamma^0 \equiv u_0, \quad u_a^a \equiv u_a, \quad u_a^{b\neq a} \equiv u_b \tag{16}$$

with

$$u_{\gamma[v]}^\alpha \equiv \langle i\chi_j^\alpha\chi_{j+v}^\alpha\rangle, \tag{17}$$

where b is a bond. u_b is set to zero for the pure Kitaev model. The resulting mean-field Hamiltonian is

$$\begin{aligned} H_{\mathrm{MF}} &= -\frac{1}{2}\sum_{i,v[i],\alpha} \mathrm{sign}[v]\nu_{\gamma[v]}^\alpha i\chi_i^\alpha\chi_j^\alpha, \\ \nu_\gamma^a &= \eta\left[(1-|\alpha|) - 2\alpha\delta_\gamma^a\right]u_0, \\ \nu_\gamma^0 &= \sum_a J_\gamma^a u_\gamma^a = \eta\left[(2-2\alpha-2|\alpha|)u_b - 2\alpha u_a\right], \end{aligned} \tag{18}$$

where J_γ^a is the coupling of spin component a on a γ-bond, i is a site, $v[i]$ are the bonds of site i and $\mathrm{sign}[v]$ is the orientation of the bond v within the PSG. This orientation determines how operators on the bond transform under symmetries. On the honeycomb, bonds are oriented from sublattice A to B. The bond orientations used in the PSGs for the triangular and the kagome lattices are depicted in Ref. [59] (though that work dealt with bosonic QSLs, the bond orientation diagrams we take are the same). For the triangle, it is known as the zero flux PSG. For the kagome, this zero flux PSG is known as $\sqrt{3}\times\sqrt{3}$ or $Q_1 = -Q_2$. The PSG analysis for this type of mean field has not been successfully carried out on the 3D lattices; the pyrochlore does not appear to give a unique decomposition [68]. On the hyperkagome, however, one of the four spins in each tetrahedra is removed, so we can consistently choose the orientation $A \to B \to C \to A$ within a triangular face in Fig. 4, giving a unique PSG (given a choice of hyperkagome chirality [33]).

The mean-field Hamiltonian H_{MF} is a free Majorana bilinear Hamiltonian, so its ground state is immediately known by computing its band structure. The qualitative properties of this band structure carry the primary information, though the band structure energy scales contain the unknown mean-field parameters u. The parameters u can be determined self-consistently from the band structure by computing the Majorana propagator, as a Matsubara frequency integral of the inverse of the frequency-dependent Hamiltonian kernel. We have carried out the self-consistency computation on the triangular and honeycomb lattice, using the Kitaev-type Majorana flux-free PSG, which is defined on these two lattices, and find that the mean fields evolve with α smoothly away from the Kitaev limit, with no first-order transitions.

Regardless of the exact values of the mean-field parameters, choosing the mean field to be analogous to the Kitaev honeycomb QSL already determines key properties of the resulting states on the various lattices. First, all the lattices except for the honeycomb possess cycles with an odd number of bonds, such as triangles; this immediately requires the Kitaev Majorana mean field to spontaneously break time-reversal symmetry [69]. These time reversal broken spin liquids might not display typical characteristics of time-reversal broken states. For example, on the triangular lattice, even though time reversal as well as $2\pi/6$ rotation each independently flip the flux pattern in triangular faces, the combined operation of time reversal with $2\pi/6$ rotation is still preserved as a single symmetry operation, so the Hall conductance vanishes. Second, lattices with an odd number of sites per unit cell necessarily have a spinon Fermi surface; the even-unit-cell lattices of pyrochlore and hyperkagome may or may not host gapped spinons.

Third, certain qualitative features of the band structure are determined by the choice of mean fields, such as the consideration of only nearest-neighbor bonds and the PSG. There are four Majorana fermion species per site; for a pure Kitaev Hamiltonian, $\chi^{1,2,3}$ have bands related to each other by the 120° SOC combined spin-spatial rotation, while χ^0 has a generally different dispersion. For the honeycomb model, χ^0 has a Majorana analogue of the Dirac cone, i.e., relativistic with zero mass, while $\chi^{1,2,3}$ all have completely flat bands separated from zero energy by a complete gap. The kagome

lattice $\chi^{1,2,3}$ also has a flat band but it lies at zero energy, i.e., at the Fermi energy, yielding the Fermi surface which necessarily arises here. The flatness results from a localized unpaired Majorana mode on one of the three sites in each unit cell; but since the remaining two sites form a line spanning the lattice, they disperse and the other bands are not flat, touching zero energy along lines in a quasi-1D spectrum. For the pyrochlore, even qualitative statements cannot be currently made, since as mentioned above, there is no special choice of minimal flux PSG. On the hyperkagome with bond orientations as described above, χ^0 has some gapless subextensively degenerate modes (such as from Γ to M), but $\chi^{1,2,3}$, like for the honeycomb, have completely flat bands. These arise, as previously mentioned, because both the honeycomb and the hyperkagome fragment into extensively many disconnected clusters when only bonds of a single Kitaev label are kept. However, while the honeycomb clusters have an even number of sites and hence can form two fully gapped bands, separated from zero energy, the hyperkagome clusters have an odd (three) number of sites; each cluster always has one energy band at zero energy and hence $\chi^{1,2,3}$ are gapless.

VII. OUTLOOK

On the honeycomb lattice, the roles of the SU(2)-symmetric Heisenberg coupling and the SOC Kitaev coupling are distinct and clear: Heisenberg exchange yields magnetic order whereas Kitaev exchange yields the exactly solvable QSL phase. The natural interpolation between the two limits, which would occur if the couplings arise in iridium oxide compounds, is consistent with this framework: the intermediate region simply holds more magnetic order. However, as we have discussed above, generalizations of the Kitaev coupling naturally arise in iridium structures and other geometries of edge-sharing octahedra on many other lattices, motivating the study of the phase diagrams of Eq. (1) on these various 2D and 3D lattices. Beyond the honeycomb, the roles of the two exchanges begin to break down.

The effect of lattice geometry on the "frustration" of a lattice is quite different for the two terms; the Hamiltonian and the lattice determine the frustration together, not independently. More surprisingly, even in cases when the Heisenberg Hamiltonian appears highly frustrating, interpolating between the AF Heisenberg and the Kitaev limits, we find a phase that occurs on *all* the lattices and which is exact and fluctuation free at a certain parameter point. Subtle interplays of different magnetic couplings, rather than a monotonic "frustration" measure, seem to be at play. The intermediate stripy phase is exact by virtue of being related to the ferromagnet, through a duality that emerges through the SOC on the t_{2g} orbitals microscopically generating the Hamiltonian.

The Klein group structure of the mapping between Hamiltonians (a duality) is in some sense highly specific to these quantum chemistry considerations but in another sense, as a mathematical object $\mathbb{Z}_2 \times \mathbb{Z}_2$, quite universal. The duality transformation it generates is interesting here for another reason: while most dualities fix a single self-dual Hamiltonian and map the two regimes on either side of that point, with qualitatively different features, to each other, the Klein duality is different. It admits two self-dual Hamiltonians, which seem to generally lie in the interior of a phase. And it acts in a complicated way on spin and spatial indices, making its action as a $\mathbb{Z}_2$ symmetry operation highly nontrivial.

Regarding possible experimental significance of Hamiltonians arising from strong SOC, it is important to observe that the Kitaev couplings naturally occur in a manner more subtle and constraining than naive symmetry considerations would suggest: for example, Kitaev interactions can arise for iridium ions on the fcc but not on the simple cubic. Computations of the quantum phase diagrams on the various lattices, especially the pyrochlore and hyperkagome, will pave the way towards predictions and comparisons with experimental results.

ACKNOWLEDGMENTS

We thank Yi-Zhuang You, Yuan-Ming Lu, George Jackeli, and Christopher Henley for useful discussions. We are also grateful for the hospitality of the Kavli Institute for Theoretical Physics, where part of this work was written. This research is supported in part by the NSF under Grants No. DGE 1106400 and NSF PHY11-25915 for the KITP Graduate Fellowship Program (IK), and ARO MURI grant W911NF-12-0461 (AV).

[1] X.-L. Qi and S.-C. Zhang, Rev. Mod. Phys. **83**, 1057 (2011).
[2] M. Z. Hasan and J. E. Moore, Annu. Rev. **2**, 55 (2011).
[3] M. Z. Hasan and C. L. Kane, Rev. Mod. Phys. **82**, 3045 (2010).
[4] D. Pesin and L. Balents, Nat. Phys. **6**, 376 (2010).
[5] X. Wan, A. M. Turner, A. Vishwanath, and S. Y. Savrasov, Phys. Rev. B **83**, 205101 (2011).
[6] G. Jackeli and G. Khaliullin, Phys. Rev. Lett. **102**, 017205 (2009).
[7] J. Chaloupka, G. Jackeli, and G. Khaliullin, Phys. Rev. Lett. **105**, 027204 (2010).
[8] G. Khaliullin, Phys. Rev. B **64**, 212405 (2001).
[9] A. Kitaev, Ann. Phys. **321**, 2 (2006).
[10] J. Chaloupka, G. Jackeli, and G. Khaliullin, Phys. Rev. Lett. **110**, 097204 (2013).
[11] J. Reuther, R. Thomale, and S. Trebst, Phys. Rev. B **84**, 100406 (2011).
[12] H.-C. Jiang, Z.-C. Gu, X.-L. Qi, and S. Trebst, Phys. Rev. B **83**, 245104 (2011).
[13] S. K. Choi, R. Coldea, A. N. Kolmogorov, T. Lancaster, I. I. Mazin, S. J. Blundell, P. G. Radaelli, Y. Singh, P. Gegenwart, K. R. Choi, S.-W. Cheong, P. J. Baker, C. Stock, and J. Taylor, Phys. Rev. Lett. **108**, 127204 (2012).
[14] X. Liu, T. Berlijn, W.-G. Yin, W. Ku, A. Tsvelik, Y.-J. Kim, H. Gretarsson, Y. Singh, P. Gegenwart, and J. P. Hill, Phys. Rev. B **83**, 220403 (2011).
[15] F. Ye, S. Chi, H. Cao, B. C. Chakoumakos, J. A. Fernandez-Baca, R. Custelcean, T. F. Qi, O. B. Korneta, and G. Cao, Phys. Rev. B **85**, 180403 (2012).
[16] A. F. Albuquerque, D. Schwandt, B. Hetényi, S. Capponi, M. Mambrini, and A. M. Läuchli, Phys. Rev. B **84**, 024406 (2011).
[17] J. Reuther, D. A. Abanin, and R. Thomale, Phys. Rev. B **84**, 014417 (2011).

[18] I. I. Mazin, H. O. Jeschke, K. Foyevtsova, R. Valentí, and D. I. Khomskii, Phys. Rev. Lett. **109**, 197201 (2012).
[19] K. Foyevtsova, H. O. Jeschke, I. I. Mazin, D. I. Khomskii, and R. Valenti, arXiv:1303.2105.
[20] I. Kimchi and Y.-Z. You, Phys. Rev. B **84**, 180407 (2011).
[21] A. V. Itamar Kimchi (unpublished).
[22] F. Trousselet, M. Berciu, A. M. Oles, and P. Horsch, Phys. Rev. Lett. **111**, 037205 (2013).
[23] H. Gretarsson, J. P. Clancy, X. Liu, J. P. Hill, E. Bozin, Y. Singh, S. Manni, P. Gegenwart, J. Kim, A. H. Said, D. Casa, T. Gog, M. H. Upton, H.-S. Kim, J. Yu, V. M. Katukuri, L. Hozoi, J. van den Brink, and Y.-J. Kim, Phys. Rev. Lett. **110**, 076402 (2013).
[24] Y. Singh and P. Gegenwart, Phys. Rev. B **82**, 064412 (2010).
[25] Y. Singh, S. Manni, J. Reuther, T. Berlijn, R. Thomale, W. Ku, S. Trebst, and P. Gegenwart, Phys. Rev. Lett. **108**, 127203 (2012).
[26] R. Comin, G. Levy, B. Ludbrook, Z.-H. Zhu, C. N. Veenstra, J. A. Rosen, Y. Singh, P. Gegenwart, D. Stricker, J. N. Hancock, D. van der Marel, I. S. Elfimov, and A. Damascelli, Phys. Rev. Lett. **109**, 266406 (2012).
[27] B. J. Kim, H. Ohsumi, T. Komesu, S. Sakai, T. Morita, H. Takagi, and T. Arima, Science **323**, 1329 (2009).
[28] B. J. Kim, H. Jin, S. J. Moon, J.-Y. Kim, B.-G. Park, C. S. Leem, J. Yu, T. W. Noh, C. Kim, S.-J. Oh, J.-H. Park, V. Durairaj, G. Cao, and E. Rotenberg, Phys. Rev. Lett. **101**, 076402 (2008).
[29] G. Cao, Y. Xin, C. S. Alexander, J. E. Crow, P. Schlottmann, M. K. Crawford, R. L. Harlow, and W. Marshall, Phys. Rev. B **66**, 214412 (2002).
[30] S. J. Moon, H. Jin, K. W. Kim, W. S. Choi, Y. S. Lee, J. Yu, G. Cao, A. Sumi, H. Funakubo, C. Bernhard, and T. W. Noh, Phys. Rev. Lett. **101**, 226402 (2008).
[31] D. Yanagishima and Y. Maeno, J. Phys. Soc. Jpn. **70**, 2880 (2001).
[32] Y. Machida, S. Nakatsuji, Y. Maeno, T. Tayama, T. Sakakibara, and S. Onoda, Phys. Rev. Lett. **98**, 057203 (2007).
[33] Y. Okamoto, M. Nohara, H. Aruga-Katori, and H. Takagi, Phys. Rev. Lett. **99**, 137207 (2007).
[34] H. Kuriyama, J. Matsuno, S. Niitaka, M. Uchida, D. Hashizume, A. Nakao, K. Sugimoto, H. Ohsumi, M. Takata, and H. Takagi, Appl. Phys. Lett. **96**, 182103 (2010).
[35] S. Yan, D. A. Huse, and S. R. White, Science **332**, 1173 (2011).
[36] H.-C. Jiang, Z. Wang, and L. Balents, Nat. Phys. **8**, 902 (2012).
[37] X. Wan, A. Vishwanath, and S. Y. Savrasov, Phys. Rev. Lett. **108**, 146601 (2012).
[38] G. Lang, J. Bobroff, H. Alloul, G. Collin, and N. Blanchard, Phys. Rev. B **78**, 155116 (2008).
[39] G. Chen and L. Balents, Phys. Rev. B **78**, 094403 (2008).
[40] We now know that even the *quantum* Hamiltonian is exactly soluble with its ground state free of fluctuations, via the Klein duality.
[41] M. R. Norman and T. Micklitz, Phys. Rev. B **81**, 024428 (2010).
[42] T. Micklitz and M. R. Norman, Phys. Rev. B **81**, 174417 (2010).
[43] J. Reuther, R. Thomale, and S. Rachel, Phys. Rev. B **86**, 155127 (2012).
[44] I. Rousochatzakis, U. K. Rössler, J. van den Brink, and M. Daghofer, arXiv:1209.5895.
[45] M. J. Lawler, H.-Y. Kee, Y. B. Kim, and A. Vishwanath, Phys. Rev. Lett. **100**, 227201 (2008).
[46] Spin exchanges with lower symmetry may even be mapped to antisymmetric Dzyaloshinskii-Moriya exchanges.
[47] G. Khaliullin and S. Okamoto, Phys. Rev. Lett. **89**, 167201 (2002).
[48] G. Khaliullin and S. Okamoto, Phys. Rev. B **68**, 205109 (2003).
[49] G. Khaliullin, Prog. Theor. Phys. Suppl. **160**, 155 (2005).
[50] In this work [49], see especially the discussions related to Fig. 1 (p. 170) and Fig. 5 (p. 194).
[51] The antiferromagnet and its Klein dual on the bipartite honeycomb are of course exceptions as well.
[52] J. M. Luttinger and L. Tisza, Phys. Rev. **70**, 954 (1946).
[53] J. M. Luttinger, Phys. Rev. **81**, 1015 (1951).
[54] P. W. Anderson, Phys. Rev. **79**, 705 (1950).
[55] T. A. Kaplan and N. Menyuk, Philos. Mag. **87**, 3711 (2007).
[56] P. W. Anderson, Phys. Rev. **83**, 1260 (1951).
[57] M. F. Lapa and C. L. Henley, arXiv:1210.6810.
[58] See Supplemental Material at http://link.aps.org/supplemental/10.1103/PhysRevB.89.014414 for details on the LTA and PSG.
[59] S. Sachdev, Phys. Rev. B **45**, 12377 (1992).
[60] E. J. Bergholtz, A. M. Läuchli, and R. Moessner, Phys. Rev. Lett. **105**, 237202 (2010).
[61] M. J. Lawler, A. Paramekanti, Y. B. Kim, and L. Balents, Phys. Rev. Lett. **101**, 197202 (2008).
[62] Y. Zhou, P. A. Lee, T.-K. Ng, and F.-C. Zhang, Phys. Rev. Lett. **101**, 197201 (2008).
[63] A. Koga and N. Kawakami, Phys. Rev. B **63**, 144432 (2001).
[64] Y.-Z. You, I. Kimchi, and A. Vishwanath, Phys. Rev. B **86**, 085145 (2012).
[65] F. J. Burnell and C. Nayak, Phys. Rev. B **84**, 125125 (2011).
[66] S. Okamoto, Phys. Rev. B **87**, 064508 (2013).
[67] X.-G. Wen, Phys. Rev. B **65**, 165113 (2002).
[68] O. Tchernyshyov, R. Moessner, and S. L. Sondhi, Europhys. Lett. **73**, 278 (2006).
[69] H. Yao and S. A. Kivelson, Phys. Rev. Lett. **99**, 247203 (2007).